Title
The Dynamics of H{sub 2} Elimination from Ethylene

Journal
Journal of Photochemistry and Photobiology A, 62(3)

Authors
Stolow, A.
Balko, B.A.
Cromwell, E.F.
et al.

Publication Date
1991-05-01

LBL-31009
Preprint

Lawrence Berkeley Laboratory
UNIVERSITY OF CALIFORNIA

Materials & Chemical Sciences Division

Submitted to the Journal of Photochemistry Photobiology

The Dynamics of H_2 Elimination from Ethylene

A. Stolow, B.A. Balko, E.F. Cromwell, J. Zhang, and Y.T. Lee

May 1991

Prepared for the U.S. Department of Energy under Contract Number DE-AC03-76SF00098

DISCLAIMER

LBL-31009

THE DYNAMICS OF H_2 ELIMINATION FROM ETHYLENE

Albert Stolow, Barbara A. Balko, Evan F. Cromwell
Jingsong Zhang, and Yuan T. Lee

Department of Chemistry
University of California

and

Chemical Sciences Division
Lawrence Berkeley Laboratory
Berkeley, CA 94720 USA

May 1991

This work was supported by the Director, Office of Energy Research, Office of Basic Energy Sciences, Chemical Sciences Division, of the U.S. Department of Energy under Contract No. DE-AC03-76SF00098.

THE DYNAMICS OF H_2 ELIMINATION FROM ETHYLENE

Albert Stolow, Barbara A. Balko, Evan F. Cromwell,
Jingsong Zhang, and Yuan T. Lee

Department of Chemistry
University of California
and
Chemical Sciences Division
Lawrence Berkeley Laboratory
Berkeley, California 94720 USA

Abstract

The dynamics of H_2 elimination in the photodissociation of ethylene at 193 nm was investigated through measurements of the translational energy distribution and rovibrational state distribution of H_2 products. Using 1,1 $D_2C{=}CH_2$ and 1,2 HDC=CDH, it was shown that both 4-centered and 3-centered elimination of H_2 could take place with an acetylene/vinylidene formation ratio of approximately two-thirds. Limited 1,2 H-migration takes place during the fragmentation, presumably through an ethylidene type structure. The relatively high rotational excitation of the H_2 fragment suggests that the transition state is not symmetric, as the two ethylene H atoms approach each other and reach the transition state one C-H bond should be significantly longer than the other. The vibrational energy distributions can be roughly characterized by a vibrational temperature of 4800K and an average translational energy, which is dependent on the rovibrational state of H_2, exceeding 20 kcal/mole.

Introduction

Unimolecular decomposition may be characterized as being either simple bond rupture reactions, in which a single bond is broken and no new bonds are formed, or as concerted decomposition reactions in which old bonds are broken as the new bonds simultaneously form[1,2]. In most cases of simple bond rupture the transition state, not having a potential energy barrier in the exit, is termed "loose". The distribution of product translational energies reflects both the lack of interaction between recoiling products and the statistical distribution of internal energies at the transition state. There is a significant lowering at the transition state of the vibrational frequency associated with the bond being broken as compared with the same frequency in the excited molecule, allowing for an essentially adiabatic treatment of other internal degrees of freedom. In a 'loose' transition state, the effective potential energy for radial separation of the products is peaked at the centifugal barrier. The distribution for translational energy release peaks at very low energies.

In the case of concerted decomposition, the transition state is termed "tight". This is the case when there is a potential barrier in the exit valley and a coupling between relative translation of the products and their internal degrees of freedom. In general, at a tight transition state, once the reaction proceeds past the transition state in the exit valley, the products formed near the top of the potential energy barrier are rapidly repelled from eachother with enhanced translational energy. In addition, certain bending vibrations of a given transition state may correlate with free rotation of the products, causing the distribution of product kinetic energies to be peaked away from zero. Of course, the concerted movement of electron density from old bonds to new during the reaction necessarily involves certain symmetry considerations[3].

The structure of the transition state predetermines the initial conditions before products separate, especially the initial vibrational excitation and repulsive energy release. Thus, a study of the product translational and internal energy distributions from concerted decompositions may yield information about the transtion state structure as well as the reaction dynamics in the exit valley. Correlations between translational and internal energy release may be revealing of the coupling between these degrees of freedom as products separate.

The concerted decompostion producing molecular hydrogen is a special case that deserves attention. Not only is it a primary process occuring in the photochemistry of many organic molecules, but it is particularily interesting for fundamental reasons. The spectroscopy of H_2 is extremely well characterized. The very large energy spacing between rovibrational quantum states implies that there will be a limited number of product states produced in a decomposition process. This allows for accurate measurement of the complete translational and internal energy distributions. Furthermore, the simplicity of the H_2 elimination from a small organic molecule should allow for *ab initio* calculation of the relevant transtion states and a detailed comparison of experiment with theory.

Ethylene Photochemistry

Ethylene is the simplest unsaturated hydrocarbon. In spite of this, the details of its UV photochemistry remain unresolved[4]. Early investigations were performed in 'bulbs' using the techniques of pulse radiolysis[5], mercury sensitization[6], flash photolysis[7] and discharge lamps[8,9,10,11,12] . The consensus was that there are two equiprobable primary reaction channels, one eliminating molecular and the other atomic hydrogen. They can be depicted as follows:

Eqn 1 a $C_2H_4 \rightarrow HC{\equiv}CH + H_2$

b $C_2H_4 \rightarrow H_2C{=}C{:} + H_2$

Eqn.2 a $C_2H_4 \rightarrow C_2H_3^{\dagger} + H$

b $C_2H_4 \rightarrow HC{\equiv}CH + 2H$

The energetics of these processes are shown in Figure 1.

The molecular decomposition appears to have two pathways: a four-centered elimination (4CE) producing the acetylene molecule - Eqn.1a, and a three-centered elimination (3CE) producing the vinylidene radical - Eqn.1b. The atomic elimination reaction may also have two pathways. The first, shown in Eqn.2a, is H atom loss from ethylene producing an energized vinyl radical. The vinyl radical may also have enough energy to spontaneously decompose, as

implied by Eqn.2b. The detection[7,13] of the vinyl radical confirmed the occurence of Eqn.2a. Early isotope substitution studies indicated that the photochemical intermediary had free rotation about the C-C bond and that all hydrogens could participate although they did not exchange. They obtained a ratio of 4CE to 3CE of 2:3. A subsequent study[14], using UV flash photolysis detected the presence of triplet vinylidene ($^3B_2$) and suggested that neither acetylene nor singlet vinyledene were primary products, in contradiction with previous work. A recent investigation[15] of ethylene photochemistry at 193nm confirmed the existence of several pathways, but was unable to elucidate them. Most recently[16], a laser induced fluorescence study of atomic elimination from the 193nm photolysis of ethylene characterized the decomposition by C-H bond rupture as being a RRKM-type following internal conversion to a vibrationally hot ground state.

The spectroscopy and excited states of ethylene have been reviewed in some detail[17]. The planar ground state is labeled N($^1A_1$). The first excited state of ethylene is labeled V($^1B_2$). The broad, diffuse V←N band system extends from 215.0nm to the first Rydberg transition at 174.4nm. The intensity rises rapidly towards shorter wavelengths. The V state of ethylene is twisted; it has a potential energy minimum for the methylene groups in a perpendicular configuration. It is capable, however, of free internal rotation for 193nm excitation. The V←N transition may be regarded as the prototype for $\pi^*\leftarrow\pi$ type transitions. The second lowest excited singlet state of ethylene is labeled Z($^1A_1$) and it is also twisted. It displays the interesting phenomenon of sudden polarization[18]; the dipole moment of this state drastically increases as the methylene groups rotate and pyramidalize. This geometry may be thought of as having *zwitterionic* character, *i.e.* $^-H_2CCH_2^+$. The point of interest here is that the V and Z states interact strongly in the twisted configuration, lending ion-pair character to the V state. A possible photochemical consequence[19] of this effect is the potentially increased facility of 1,2 H atom shift, analogous to the well known 1,2 carbonium shift. A recent VUV resonance Raman study[20] of the V state confirmed that the intial motions on the excited state are CH_2 twisting and pyramidalization.

A considerable amount of theoretical work has been done relating to the problem of ethylene photochemistry. A seminal study[21] of the energetics and

symmetry allowed correlations of various states of ethylene presented important conclusions, discussed below.

The V state of ethylene correlates *directly*, with small barrier, to both the singlet ground state of vinylidene (H_2C=C:) plus H_2 and the singlet ground state of ethylidene ($HCCH_3$) as shown:

Eqn.3 $C_2H_4\,[V(^1B_2)] \rightarrow H_2C{=}C{:} + H_2$

Eqn.4 $C_2H_4\,[V(^1B_2)] \rightarrow HCCH_3$

The process shown in Eqn.3, the ethylene to vinylidene transformation, is Woodward-Hoffmann forbidden for C_{2v} symmetry and only becomes allowed for C_s symmetry, suggesting that the transition state for this path is of low symmetry. This path is not necessarily a *statistical* unimolecular decompostion.

The reaction shown in Eqn.4 would correspond to a 1,2 H atom shift and is related to the sudden polarization phenomenon. The 'ethylidene radical' was found to be completely unstable[22] with respect to rearrangment to ethylene; it is merely a saddle point on the ethylene ground state surface. There is, however, an 'ethylidene-type' transition state that leads directly[21,22] to ground state acetylene plus H_2.

Eqn.5 $HCCH_3^{\ddagger} \rightarrow HC{\equiv}CH + H_2$

It should be pointed out that the available energy of 148kcal/mol (*i.e.* 193nm) far exceeds the barriers in the ground state for H_2 elimination from vinylidene, acetylene or 'ethylidene'. The observation of the vinyl radical in Eqn.2 is confirmation of internal conversion to the hot ground state of the ethylene molecule since the V state doesn't correlate directly with the atomic elimination channel. The H atom is expected to eliminated through unimolecular decay with a few kcal/mol of the exit barrier potential energy.

Experimental

Two experimental techniques used in the study of ethylene photochemistry at 193nm will be discussed in the following sections. The first,

the molecular beam Photofragment Translational Energy Spectroscopy (PTS)[23], provides the detailed kinetic energy distributions of mass selected photolysis products and branching ratios between competing channels. The second, a VUV laser-based Pump-and-Probe technique[24] provides rotational and vibrational energy distributions for the H_2 product as well as the dependence of the average product translational energy on the rovibrational quantum state of H_2.

•Photofragment Translational Energy Spectroscopy

The experimental apparatus used in these high resolution photofragmentation studies has been described previously[25]. Briefly, an unskimmed pulsed supersonic molecular beam is expanded into a differentially pumped vaccum chamber where it is crossed at right angles with the 193nm output (500-1500mJ/cm^2) of an ArF excimer laser. Recoiling photofragments pass into a separate chamber where they are detected, after travelling a distance of 39cm, by a multiply differentially pumped rotating mass spectrometer detector. In this particular case, because the products have an isotropic angular distribution in the center-of-mass coordinate system, and that the velocities of the H and H_2 fragments so exceed the velocity of the parent molecule, the entire product translational energy distribution may be collected at a single angle, perpendicular to the plane containing the photolysis laser and the molecular beam. Transient signals at a given charge-to-mass ratio are captured and signal averaged by a computer-controlled multichannel scaler system. The product translational energy distributions are extracted from the raw data using the forward convolution technique[26].

•VUV Laser Pump-and-Probe Technique

The ultra-high resolution VUV-XUV laser system and molecular beam apparatus used in these experiments has been described previously[27,28]. The relative populations of H_2 rovibrational states are probed via (1+1) resonance enhanced multiphoton ionization (REMPI) through either the $B(^1\Sigma_u)$ or $C(^1\Pi_u)$ states[29]. In addition, the inherent high resolution of the laser allows the Doppler profiles of the H_2 transitions to be scanned, permitting an analysis of the correlations between product translation and internal energy.

A skimmed, differentially pumped, pulsed molecular beam was expanded into a vacuum chamber where it passed through the extraction region of a Wiley-McLaren type t-o-f mass spectrometer. There it was crossed by the 193nm output (10 - 80mJ/cm^2) of an unstable resonator ArF excimer laser. Collinear and counterpropagating with this were the VUV+UV probe laser beams which interrogated the nascent H_2 photoproducts at a time delay of 20ns.

The probe laser system, described in detail elsewhere[24,27], is based upon pulsed amplification of a ring dye laser. Typically, over 100mJ/pulse of visible light is produced with a bandwidth of 95MHz. This is doubled and then converted to VUV-XUV by either tripling or sum-frequency mixing in a pulsed free jet expansion of Argon or Xenon. Laser powers were monitored on a shot-to-shot basis in order to accurately normalize the collected signals. Doppler spectra were recorded by scanning the ring laser under computer control. The same laser system also allowed for the detection of H and D atom photoproducts via (1+1)REMPI (using the Lyman-α transition) by tripling in a pulsed free jet of Krypton gas.

Normalized H_2^+ signals are fitted to a lineshape function and converted to relative populations using the well known H_2 line strength factors.

Results and Discussion

Photofragment Translational Energy Spectroscopy

•Molecular Hydrogen Elimination

The H_2 product time-of-flight spectrum for ethylene photolysis is shown in Figure 2. The product translational energy distribution, $P(E_t)$, which fits this spectrum is shown in Figure 3. The maximum in the $P(E_t)$ is peaked away from zero, consistent with a concerted elimination process.

Were 4CE of H_2 to form nascent acetylene, as in Eqn. 1a, the only process, the maximum translational energy would be about 108kcal/mol. On the other hand, if 3CE of H_2 to form nascent vinylidene, as in Eqn. 1b, were the only

process, the maximum translational energy would be about 64kcal/mol. The observed maximum translational energy was 88kcal/mol, confirming the occurence of 4CE. It does not, however, indicate the absence of 3CE. In fact, the abrupt change in slope (near 60kcal/mol in Figure 3), usually indicating the presence of another channel, is suggestive of 3CE.

In order to confirm the presence of both 3CE and 4CE, it was necessary to study the elimination of HD and D_2 from two isotopically substituted ethylenes: namely (1,1) $D_2C{=}CH_2$ and cis (1,2) HDC=CDH. The experimentally observed product ratios can be self-consistently related to the branching ratio for 3CE over 4CE.

The measured relative yields of HD and D_2 from the (1,1) and cis (1,2) isotopomers are given in Table 1. The first important point is that the four hydrogen atoms are not equivalent - they do not get completely scrambled. If they did then equal amounts of HD and D_2 would be formed for each isotopomer, which is not the case. The second important point is that 4CE cannot be the only channel. If this were true, it would be impossible to form D_2 from the (1,1) isotopomer. A simple model[25] for molecular elimination allowed for an estimation of the expected HD/D_2 ratios for the case of pure 3CE and for pure 4CE from each isotopomer. Deviation from these limiting cases was used to obtain the branching ratio. It was found that the 3CE (forming viylidene) to 4CE (forming acetylene) for H_2 from the 193nm photolysis of ethylene was 2:3.

Eqn.6 $$4CE\ (HC{\equiv}CH) : 3CE\ (H_2C{=}C{:}) = 2 : 3$$

The relationship expressed in Eqn.6 can be used to extract separate translational energy distributions for 3CE and 4CE in each isotopomer. In the analysis[25] of HD elimination from the (1,1) isotopomer (forming acetylene) and D_2 from the same (forming vinylidene), it was discovered that, while the acetylene 4CE channel creates more energetic product as expected, the vinylidene 3CE channel seems to produce product with up to 78kcal/mol in translation. This exceeds the available energy for vinylidene formation of 64kcal/mol. This may provide some preliminary evidence for the contribution of an ethylidene-type mechanism. As the D_2 molecule is forming in the energized (1,1) isotopomer, an H atom from the adjacent carbon starts to transfer over, enhancing the repulsive force on the departing D_2.

•Atomic Elimination

An estimation of the branching ratio between atomic versus molecular elimination may be procured from a consideration of the integrated TOF spectra for H and H_2 generated in the photolysis of C_2H_4. The branching ratio was 1.0 ± 0.15 over the range of laser intensities from 800-1500 mJ/cm^2. The shape, however, of the H atom TOF spectra depended strongly on laser intensity. The leading edges of all spectra corresponded to a translational energy exceeding that expected from a consideration of accepted C-H bond strengths in ethylene[30]. This suggested that multiphoton effects contribute to the H atom elimination channel. A likely scenario is secondary absorption by the nascent vinyl radical (which has an absorption cross section much larger than that of ethylene at 193nm). This will be discussed in greater detail in a following section.

The primary and secondary channels may be deconvoluted[31] and the $P(E_t)$ for the primary channel extracted. This, shown elsewhere[25], peaks near zero kinetic energy and is consistent with simple bond rupture in a hot ground state ethylene molecule, producing the vinyl radical. The secondary dissociation channels can be divided into two groups[25]. The first is spontaneous decomposition of the over-energized vinyl radical into acetylene plus an H atom with 0-5kcal/mol in translation. The second H atom elimination channel is considered to be photodissociation of the nascent vinyl radicals (including a large fraction of over-energized species), producing very fast H atoms. The analysis of this secondary $P(E_t)$ suggests that electronically excited molecular products are formed. In particular, the $P(E_t)$ has a threshold (approx. 100kcal/mol) close to that expected for forming triplet vinylidene, $H_2C{=}C{:}$ ($^3B_2$). This point is supported by a previous study[14] of ethylene photochemistry in which the direct observation of $^3B_2$ vinylidene was reported.

VUV Pump-and-Probe Technique

•Product State Distributions

The vibrational state distribution of H_2 product from the 193nm photodissociation of C_2H_4 is shown in Figure 4. The detailed rotational distributions for vibrational levels v = 0 - 3 are given in Figure 5. The populations were determined from the normalized Doppler scans by fitting to a lineshape function, extracting the line intensity and converting this to a population by using the well known H_2 line strength factors. Each population was measured 4-6 times, using P, Q and R transitions whenever possible.

The rotational distributions for H_2 elimination from the (1,1) dideuterated isotopomer were measured for v = 0 and v = 1. These have been interpreted as arising from a pure 3CE mechanism. The distributions were fit to rotational 'temperatures' of 2500 ± 200K for v = 0 and 2000 ± 160K for v = 1. The important point here is that these distributions are significantly rotationally cooler than for those for H_2 from C_2H_4.

In order to deconvolute the rovibrational distributions for 3CE and 4CE channels, two major assumptions were required. The first was that the overall branching ratio between 4CE and 3CE is 2:3, as obtained from the above-mentioned molecular beam TOF studies. The second was that the vibrational 'temperature' for 3CE was *one-half* that for 4CE. This was based on the observation that the exothermicity for 3CE is approximately one-half that for 4CE and is in accordance with the rotational temperature for 3CE obtained from the (1,1) dideuterated isotopomer study mentioned above. From these assumptions we estimated the bimodal vibrational distribution, shown in the first column of Table 2.

For the vibrational levels v = 0 and v = 1, it was possible to directly deconvolute the 4CE rotational distribution since the 3CE rotational distribution was known from the (1,1) isotopomer photolysis discussed above. For the v = 2 and v = 3 levels, the two rotational temperatures were varied to best fit the observed data with the constraint that the ratio of 3CE to 4CE matched the vibrationally resolved branching ratio from the first column of Table 2. The derived rotational temperatures for the two elimination channels are shown, as a function of v-level, in Table 2.

Several points are worth noting. The bimodal fit to the vibrational distribution shows the fraction of 3CE decreasing from nearly 70% in v = 0 to less than 20% in v = 3. The rotational temperatures for 3CE are consistently much cooler than those for 4CE. These differences can be understood primarily in terms of the energy available to each channel (4CE has twice as much). The highly rotationally excited products from 4CE are suggestive of a quite asymmetric transition state wherein the two recoiling H atoms, on their way to forming an H_2 molecule, experience unequal repulsive forces. In the case of 3CE, the rotational temperatures, though cooler, are still much hotter than those observed for the recoil of H_2 from a highly symmetric transition such as found in the photolysis of 1,4 cyclohexadiene[32]. This suggests the pure 3CE case also has an asymmetric transition state, perhaps analogous to the well known case of H_2 elimination from formaldehyde[33]. It may also be suggestive of some contribution from an ethylidene-type component in the 3CE transtition state, where the H atom from the adjacent carbon starts transferring over as the H_2 departs.

•Correlations with Translational Energy

The lineshape for each H_2 (v,J) transition was fitted to a functional form[34] by assuming that a Gaussian distribution of velocities contribute to the Doppler profile[35,24]. From these fits, average and maximal translational energy releases may be correlated with H_2 product internal energies. A plot of the H_2 average translational energy as a function of H_2 internal energy is shown in Figure 6. As expected, the translational energy decreases with increasing internal energy - consistent with fixed available energy. There is not, however, a simple antagonistic relationship between translational and internal energy: the translational energy falls off *much* less quickly. This is consistent with the picture of a tight transition state where the partitioning to translation is governed by product repulsion in the exit valley.

Ethylene contains so many degrees of freedom (*i.e.* 12) and the excitation energy (*i.e.* 148kcal/mol) so exceeds the exit barrier energy that dissociation could take place from a range of structures near the transition state. This is because the

excess energy must get distributed in modes other than the reaction coordinate, leading to vibrationally excited transition states which have a range of geometries about the true structure at the minimum energy barrier (saddle point). Furthermore, these excess energy structures may 'see' slightly different exit barriers than the minimum energy transition state. Therefore, the H_2 translational, rotational and vibrational distributions and their mutual correlations reveal information not only about the structure of the transition state but also the *range* of structures from which the C_2H_4 molecule dissociates.

The H_2 average translational energy may also be correlated with rotational energy for each vibrational state. In these plots, shown elsewhere[35], the translational energy release shows a weak negative correlation with H_2 rotational energy. This observation allows us to speculate further upon the dynamical origins of these highly rotationally excited products. The extensive rotational excitation could be dominated by either the increased magnitude (*i.e.* the height of the exit barriers for various critical structures near the transition state) or increased anisotropy (*i.e.* asymmetry at the transition state) of the repulsive forces. If the increased magnitude dominated, one would expect a *strong* negative correlation between product translation and product rotation as one is traded off for the other. On the other hand, if increased anisotropy dominated, we would expect a *weak* negative correlation. This is so because the translational energy, governed by the magnitude of the potential energy released beyond the transition state, should be relatively independent of the rotational energy, having arisen from asymmetry at the transition state. Therefore, if anisotropic forces govern the extent of rotational excitation, the correlation between translation and rotation should be weak. This is consistent with our observations. The correlation appears to be slightly weaker for higher v-levels rather than low. If this is true, it may suggest that the dominance of the repulsive anisotropy is more important for the case of 4CE.

It is interesting to compare the Doppler profiles for H_2 (v = 0,1) elimination from the (1,1) isotopomer with those from regular ethylene. The negative correlation between product translation and product rotation is considerably stronger for the (1,1) isotopomer. This is most likely to be explained by the contribution of the rotationally hotter 4CE in C_2H_4 (absent in the (1,1) isotopomer), weakening the correlation. However, 4CE contributes only about

30% to the v = 0 rotational distribution in C_2H_4 (see Table 2). It might also be that in 3CE from the (1,1) isotopomer, there is a stronger translational-rotational correlation than in 3CE from C_2H_4. If this is true, it might have some bearing on the structure of the transition state for 3CE. If the anisotropy of the repulsion in the 3CE transition state is due to the transferring over of an H atom during recoil, one might expect that the transfer of a D atom is much less likely, reducing the anisotropy and therefore strengthening the negative correlation. This would be consistent with the observation of faster than expected 3CE product obtained in the comparison of HD with D_2 in the (1,1) isotopomer, as discussed in the molecular beam technique section above.

An investigation into the distribution of H_2 velocities for a single rovibrational state was carried out using the technique of Velocity Aligned Doppler Spectroscopy (VADS)[36]. This technique allows for enhanced resolution at long time delays in the determination of different velocity components contributing to a Doppler lineshape. Doppler scans for three different $H_2(v,J)$ states are shown in Figure 7. The lineshapes are split symmetrically about line center and peak at finite Doppler shifts. This indicates that the average translational energy release is peaked away from zero, in good agreement with the molecular beam TOF data, and consistent with the picture of a tight transition state. The significant width of the peaks indicates that each $H_2(v,J)$ correlates with a large distribution of internal energies in the hydrocarbon fragment. This is not unanticipated as a consideration of the energy partitioned to the H_2 fragment reveals that this must be the case. We had hoped that the Doppler profiles would show a bimodal velocity distribution, indicating two competing elimination channels. Preliminary evidence for this appeared in a long time delay scan of the lineshape for a $H_2(v = 2, J = 1)$ transition, shown in Figure 8. There is a narrower, slower velocity distribution superimposed on a broader one. The maximum Doppler shift in the broad component corresponds to a translational energy of 46kcal/mol. Considering the internal energy of this H_2 state (23kcal/mol), the broad peak must correspond to 4CE forming acetylene since 3CE is no longer thermodynamically possible at this high energy. Therefore, we associate the narrower, slower peak with 3CE and the broader peak with 4CE. The ratio of the areas of the broad and narrow peaks is roughly 2:1, in agreement with the bimodal vibrational distribution for a v=2 state, as shown in Table 2.

•Atomic Elimination and Multiphoton Processes

A study of the atomic elimination channel in the 193nm photodissociation of ethylene was procured by measuring the Doppler profiles of D atoms produced from C_2D_4. A typical Doppler lineshape for D atom elimination is shown in Figure 9. It is peaked at zero Doppler shift for all time delays and is considerably narrower than the Doppler profiles for molecular hydrogen elimination. This indicates that the distribution of translational energies is peaked near zero, supporting the molecular beam TOF data and consistent with a simple bond rupture process. The average translational energy release from a long time delay Doppler scan[25] was measured to be around 7.8kcal/mol, in general agreement with a prior study[16].

An analysis of the maximum Doppler shift, however, reveals that multiphoton processes must be occuring. The maximum shift from Figure 9 corresponds to a translational energy greater than 70kcal/mol. There probably is faster product yet, as seen in the TOF data, but the ion collection becomes less efficient as the energy increases, reducing our sensitivity for the very fastest products. Even so, if interpreted as simple bond rupture in C_2D_4, it would suggest a C-D bond energy of 78kcal/mol, far below accepted values[30]. The recoiling D atom has far too much energy for a single photon process. This is consistent with nascent vinyl radical absorbing a second photon, producing a very fast D atom and triplet vinylidene.

That there are multiphoton processes is not unexpected if one considers the relative photoabsorption cross sections of the ethylene molecule and the vinyl radical. The UV cross section of ethylene[17] is very small, around 2×10^{-20} cm^2. The UV cross section of the vinyl radical, on the other hand, is much greater[37]. Thus, as the laser intensity is increased to produce measurable signal from the photolysis of ethylene, it becomes very difficult to avoid secondary dissociation of the vinyl radical product.

We performed laser power studies on the D atom product. With the VUV probe laser set to zero Doppler shift (the Lyman-α line center), we obtained a straight line fit to the data, passing through the origin, over the range of laser intensities from 50-100mJ/cm^2. This cannot, however, be taken as evidence that

multiphoton processes do not occur since the leading edge of the Doppler profile confirms that they do. In a second study, we set the VUV probe laser far off line center, near the red edge of the Doppler scan, corresponding to a translational energy release that must involve multiphoton processes. This is presented in Figure 10. At low laser intensities, from 30 to 60mJ/cm^2, we can see a non-linear response. Above 100mJ/cm^2, the data is well represented by a straight line. This suggests that multiphoton processes can occur in ethylene photochemistry and saturate at relatively low intensities due to the very large absorption cross section of the vinyl radical as compared to the parent molecule.

Summary

The photochemistry of ethylene (C_2H_4) at 193nm has been studied by two complementary techniques: molecular beam Photofragment Translational Energy Spectroscopy and the VUV-XUV Pump-and-Probe technique. The former determined product translational energy distributions and branching ratios while the latter determined H_2 product rotational and vibrational energy distributions. Prior experimental and theoretical work suggested that there might be two pathways to molecular H_2 elimination. The first, called three-centered elimination (3CE), brings together two H atoms from the *same* carbon to form H_2, leaving behind the vinylidene radical (H_2C=C:). The second, called four-centered elimination (4CE), brings together H atoms from *different* carbons, leaving behind the acetylene molecule (HC≡CH). The 4CE channel is nearly twice as exothermic as the 3CE channel.

The elimination of H and of H_2, shown in Eqns.1 & 2, were found to occur in a 1:1 ratio, in agreement with previous investigations. Isotopic substitution studies of molecular hydrogen elimination using (1,1) dideuteroethylene and cis (1,2) dideuteroethylene revealed that the ratio of 4CE to 3CE in C_2H_4 was 2:3, also in agreement with previous investigations. The translational energy distributions for H_2 elimination were peaked *away* from zero, indicating a concerted decomposition process from a tight transition state. Translational energy distributions for H atom elimination, leaving the vinyl radical, were

found to peak near zero. This suggests that excited ethylene internally converts to form a hot ground state which then undergoes a simple bond rupture, forming the vinyl radical and an H atom. The vinyl radicals appears to have enough internal energy to spontaneously decompose, forming acetylene plus a slow H atom. Based upon the observation of very fast H atoms, secondary photolysis of the vinyl radical was postulated, forming, perhaps, a triplet vinylidene radical.

The vibrational distribution for H_2 elimination from C_2H_4 corresponded to a high temperature, near 5000K. The contibution of 3CE was estimated to be nearly 70% for v = 0, decreasing to less than 20% for v = 3. The H_2 rotational distributions for each v-level extended to high J levels. Separate rotational distributions were extracted for 3CE and 4CE; the former was significantly cooler at each v-level than the latter. The high degree of rotational excitation is suggestive of asymmetry in the transition states. Correlations between translational and rotational energy were obtained by measuring the Doppler profiles of the H_2 transitions. There was a weak negative correlation between translation and rotation, suggesting that perhaps asymmetry in the transition states dominates over repulsive energy release in the determination of the degree of rotational excitation. When two H-atoms are pushed together as the energized molecule approaches the transition state, one C-H bond is significantly longer than the other. The *negative* correlation between translational and internal energy further suggests that the *range* of transition state structures (determining the energies available to the departing H_2) is mainly due to variation in the *longer* C-H bond distance near the transition state.

An analysis of the Doppler lineshapes supported the picture of a concerted dissociation process producing H_2. Preliminary evidence for the presence of two velocity distributions in a given lineshape was presented, consistent with the competition between 3CE and 4CE. The atomic elimination channel was studied by observing D atom elimination from C_2D_4. The translational energy distribution peaked at zero, corroborating the molecular beam data and the notion of simple bond rupture in a hot ground state molecule. Evidence for the occurence of multiphoton processes, based upon laser power studies at a large D atom Doppler shift, was presented and interpreted in terms of the secondary dissociation of vinyl radicals.

The transition state for 3CE should be asymmetric, with two unequal C-H bond distances for the departing H atoms, perhaps analogous to the formaldehyde case. There may also be some concerted interaction with an H atom from the adjacent carbon. The transition state for 4CE should be quite asymmetric, perhaps passing near an ethylidene-type structure. However, incomplete scrambling of the hydrogens implies that this contribution is also limited. It seems that a range of structures about the transition state saddle point should participate in the dissociation; the most likely geometrical variation involving changes in the longer of the two C-H bond distances concerned. We hope that these results will stimulate new theoretical investigations into the dynamics of concerted decomposition in ethylene.

Acknowledgements.

This work was supported by the Director, Office of Basic Energy Sciences, Chemical Sciences Division of the U.S. Department of Energy under contract No. DE-ACO3-67SF00098. A.S. would like to acknowledge NSERC (Canada) for the receipt of a postdoctoral fellowship.

Figure Captions

Table 1. Relative amounts of HD and D_2 product formed in the photolysis of (1,1) $D_2C{=}CH_2$ and cis (1,2) HDC=CDH. The yields are normalized to the yield of HD product from the (1,1) isotopomer.

Table 2. Bimodal fit to 3CE and 4CE for the H_2 rotational distributions in the photolysis of C_2H_4. Shown are the rotational temperature for 3CE and 4CE as a function of vibrational state. Also shown is the percentage 3CE contributing to the total signal at each v-level.

Figure 1. Heats of reaction of various species involved in ethylene photochemistry. The photon energy is 148kcal/mol (*i.e.* 193nm). Many of the heats of formation are not well known. The values used here are discussed in reference 25.

Figure 2. H_2 TOF spectrum from photolysis of C_2H_4 at a 193nm laser power of 130mJ/pulse. The solid line is the best fit calculated using the $P(E_t)$ shown in Figure 3.

Figure 3. $P(E_t)$ for H_2 formation used to fit the TOF spectrum shown in Figure 2. The arrows indicate the maximum H_2 translational energies expected for acetylene, vinylidene, excited state acetylene and excited state vinylidene formation.

Figure 4. Distribution of vibrational energy in H_2 from the photodissociation of C_2H_4 (solid bars). A statistical fit to the data (with T = 4979 ± 120K) is also shown (hatched bars).

Figure 5. Detailed H_2 rotational distributions for v = 0 - 3. Errors bars indicate one standard deviation.

Figure 6. Plot of translational energy versus internal energy for H_2 product from the photodissociation C_2H_4. The vibrational quantum states of the H_2 product are indicated.

Figure 7. H_2 Doppler profiles measured by VADS for the v = 1 level. Top: H_2 B←X(2,1) R(5) transition, ν_0 = 87710.0 cm^{-1}. Middle: H_2 B←X(2,1) P(3) transition, ν_0 = 88077.1 cm^{-1}. Bottom: H_2 B←X(2,1) R(1) transition, ν_0 = 87358.2 cm^{-1}. The VADS profiles are shown in a heavy line while the normal Doppler profiles are shown with a light line, scaled down to match the VADS intensity.

Figure 8. Red edge of the VADS profile for the H_2 B←X(2,1) R(5) transition, (ν_0 = 87710.0 cm^{-1}) at a 700ns time delay. A narrow velocity distribution (3CE) appears superposed on a broader one (4CE). The ratio of broad-to-narrow is 2:1, consistent with the 4CE-to-3CE at v = 2, as shown in Table 2.

Figure 9. Doppler profile for D atoms from C_2D_4 photodissociation. The dashed line shows the maximum Doppler shift expected for single photon excitation of C_2D_4 forming a D atom plus vinyl radical. Signal to the left of the dashed line must come from a multiphoton process.

Figure 10. 193nm photolysis laser intensity study with the VUV probe laser set at a H_2 Doppler shift shown by the dashed line in Figure 8. The behaviour at low intensity appears non-linear (indicating multiphoton absorption), saturating at higher intensities where it is well approximated by a straight line.

References

1 F.Huisken, D.Krajnovitch, Z.Zhang, Y.R.Shen & Y.T.Lee, J.Chem.Phys. 78, 3806 (1983); D.Krajnovitch, F.Huisken, Z.Zhang, Y.R.Shen & Y.T.Lee, *ibid*, 77, 5977 (1982).

2 R.A. Marcus, *ibid*, 62,1372 (1975); G.Worry & R.A.Marcus, *ibid*, 67, 1636 (1977) ; S.A.Safron, N.D.Weinstein & D.R.Herschbach, Chem.Phys.Lett. 12, 564 (1972).

3 R.Hoffmann & R.B.Woodward, Angew.Chem.Int.E.Eng. 8, 781 (1969)

4 G.J.Collin, Adv.Photochem. 14, 135 (1988)

5 R.Gorden &P.Ausloos, J.Res.Nat.Bur.Std.Sec.A 75A, 141 (1971); P.Ausloos & R.Gorden, J.Chem.Phys. 36, 5 (1961)

6 A.B.Callear & R.J.Cvetanovic, *ibid*, 24, 873 (1955)

7 R.A.Back & D.W.L.Griffiths, *ibid*, 46, 4839 (1967)

8 M.C.Sauer & L.M.Dorfman, *ibid*, 35, 497 (1961)

9 H.Okabe & J.R.McNesby, *ibid*,36, 601 (1962)

10 E.Tschuikow-Roux, J.R.McNesby, W.M.Jackson & J.L.Faris, J.Phys.Chem. 71, 1513 (1967)

11 P.Borrel, A.Cervanka & J.W.Turner, J.Chem.Soc.(B), 2293 (1971)

12 H.Tara & I.Tanaka, Bull.Chem.Soc.Jpn. 46, 3012 (1973)

13 H.Tara & I.Tanaka, *ibid*,47, 1543 (1974)

14 A.Fahr & A.H.Laufer, J.Photochem. 34, 261 (1986); A.H.Laufer, *ibid*, 27, 267 (1984)

15 L.Giroux, M.H.Back & R.A.Back, Can.J.Chem. 67, 1166 (1989)

16 S.Satyapal, G.W.Johnston, R.Bersohn & I.Oref, J.Chem.Phys. 93, 6398 (1990)

17 A.J.Merer & R.S.Mulliken, Chem.Rev. 69, 639 (1969)

18 R.J.Buenker, V.Bonacic-Koutecky & L.Pogliani, J.Chem.Phys.73, 1836 (1980)

19 W.Cherry, M.F.Chow,M.J.Mirbach, M.F.Mirbach, V.Ramamurthy & N.J.Turro, J.Mol.Photochem. 8, 175 (1977)

20 R.J.Sension & B.J.Hudson,J.Chem.Phys. 90,1377 (1989)

21 E.M.Evleth & A.Sevin, J.Am.Chem.Soc. 103,7414 (1981) *& references therein.*

22 K.Raghavachari, M.J.Frisch, J.A.Pople & P.v.R.Schleyer, Chem.Phys.Lett. 85, 145 (1982)

23 A.M.Wodtke, PhD Thesis, U.C.Berkeley (1986)

24 E.F.Cromwell, PhD Thesis, U.C.Berkeley (1991)

25 B.A.Balko, J.Zhang & Y.T.Lee, *to be published.*

26 X. Zhao, PhD Thesis, U.C.Berkeley (1988)

27 E.F.Cromwell, T.Trickl, Y.T.Lee & A.H.Kung, Rev.Sci.Instr. 60, 2888 (1989)

28 E.F.Cromwell, D.J.Liu, M.J.J.Vrakking, A.H.Kung & Y.T.Lee, J.Chem.Phys. *in press*

29 A.H.Kung, T.Trickl, N.A.Gershenfeld & Y.T.Lee, Chem.Phys.Lett.144,427 (1988)

30 K.M.Ervin, S.Gronert, S.E.Barlow, M.K.Gilles, A.G.Harrison, V.M.Bierbaum, C.H.DePuy, W.C.Lineberger & G.B.Ellison, J.Am.Chem.Soc. 112, 5750 (1990)

31 X.Zhao, PhD Thesis, U.C.Berkeley (1988)

32 E.F.Cromwell, D.-J.Liu, M.J.J.Vrakking, A.H.Kung and Y.T.Lee, J.Chem.Phys. *in press.*

33 T.J.Butenhoff, K.L.Carleton & C.B.Moore, J.Chem.Phys. 92, 377 (1990)

34 R.N.Dixon, *ibid*, 85, 1866 (1986)

35 E.F.Cromwell, A.Stolow, M.J.J.Vrakking & Y.T.Lee, *to be published.*

36 Z.Xu, B.Koplitz & C.Wittig, J.Chem.Phys. 87, 1062 (1987)

37 A.Fahr & A.H.Laufer, J.Phys.Chem 92, 7229 (1988)

TABLE 1. : Relative Product Yields from Isotopomer Photolysis		
Isotopomer	**D_2 (m/e = 4)**	**HD (m/e = 3)**
(1,1) $D_2C{=}CH_2$	0.5	1.0
cis (1,2) HDC=CDH	0.2	2.0

Table 1

TABLE 2. : Bimodal Fit to H_2 Rotational Distributions			
Vibrational State	**%3CE**	**T_{rot}(3CE)**	**T_{rot}(4CE)**
0	67	2500±200K	3500±940K
1	49	2000±160K	4200±800K
2	32	1200	4000±1200K
3	19	600	2700±350K

Table 2

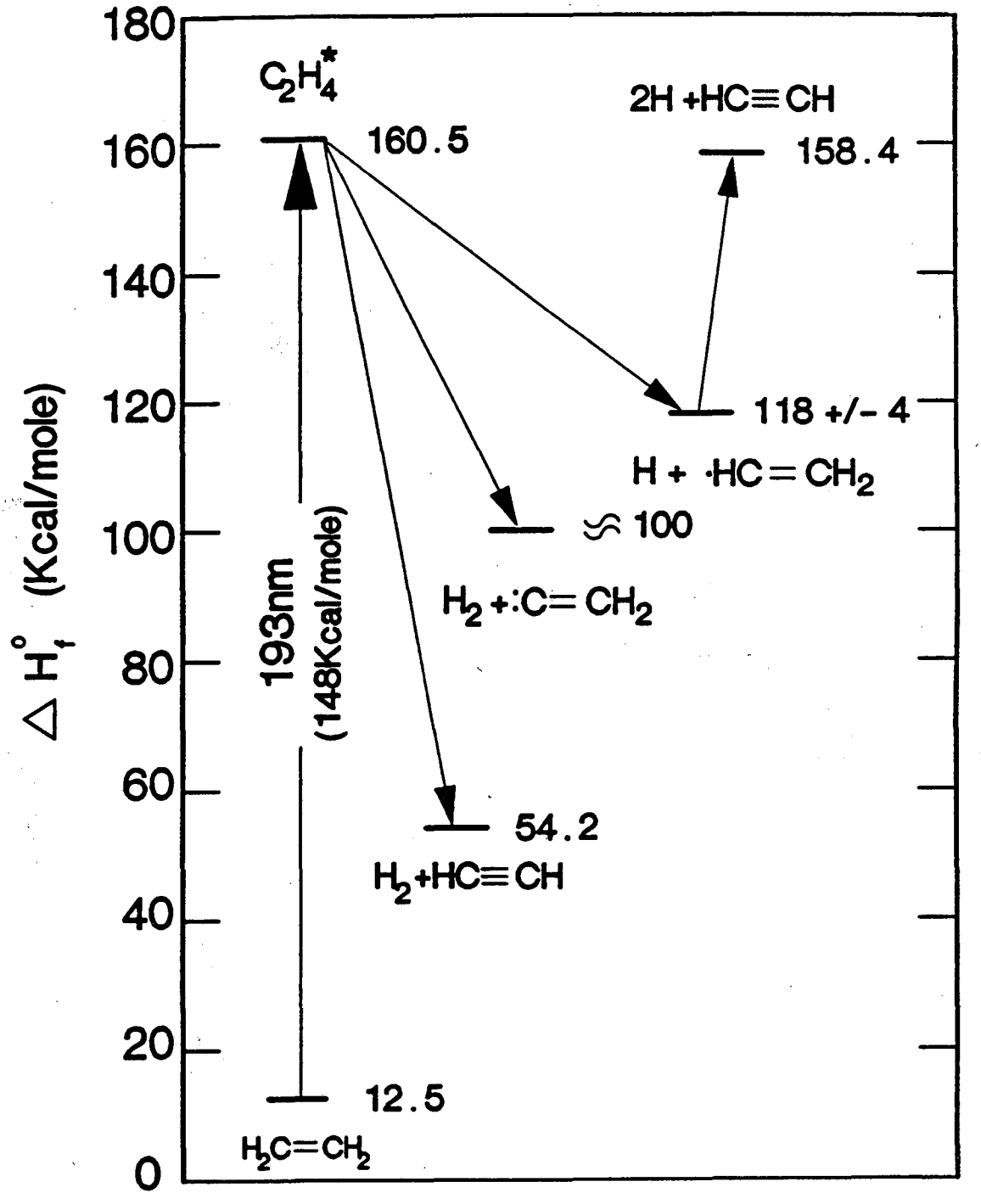
180
160
140
120
100
80
60
40
20
0
ΔH_f° (Kcal/mole)
$C_2H_4^*$
160.5
2H + HC≡CH
158.4
118 +/- 4
H + ·HC=CH$_2$
≲ 100
H_2 + :C=CH$_2$
193nm
(148Kcal/mole)
54.2
H_2+HC≡CH
12.5
H_2C=CH$_2$

Figure 1

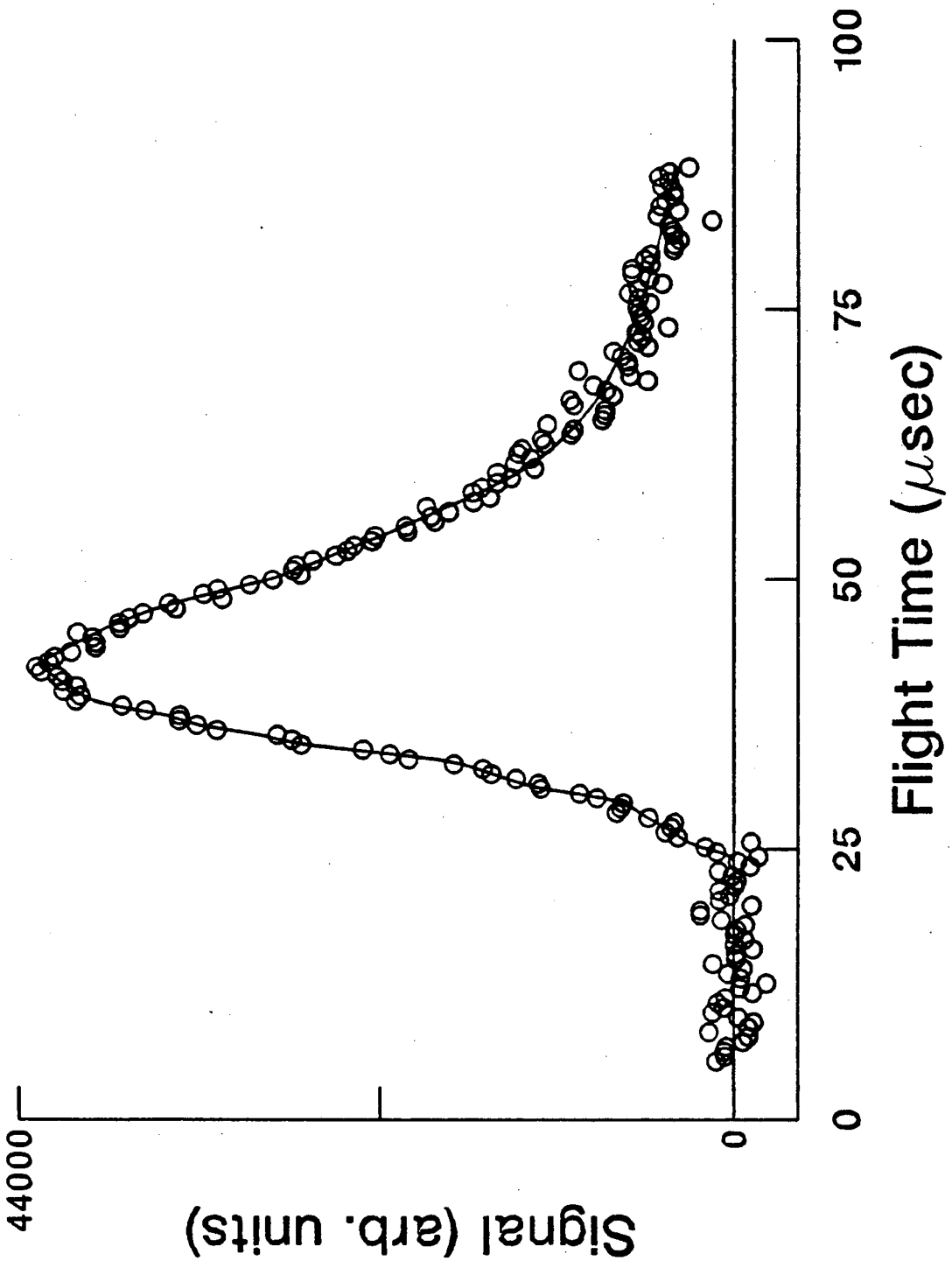

Figure 2

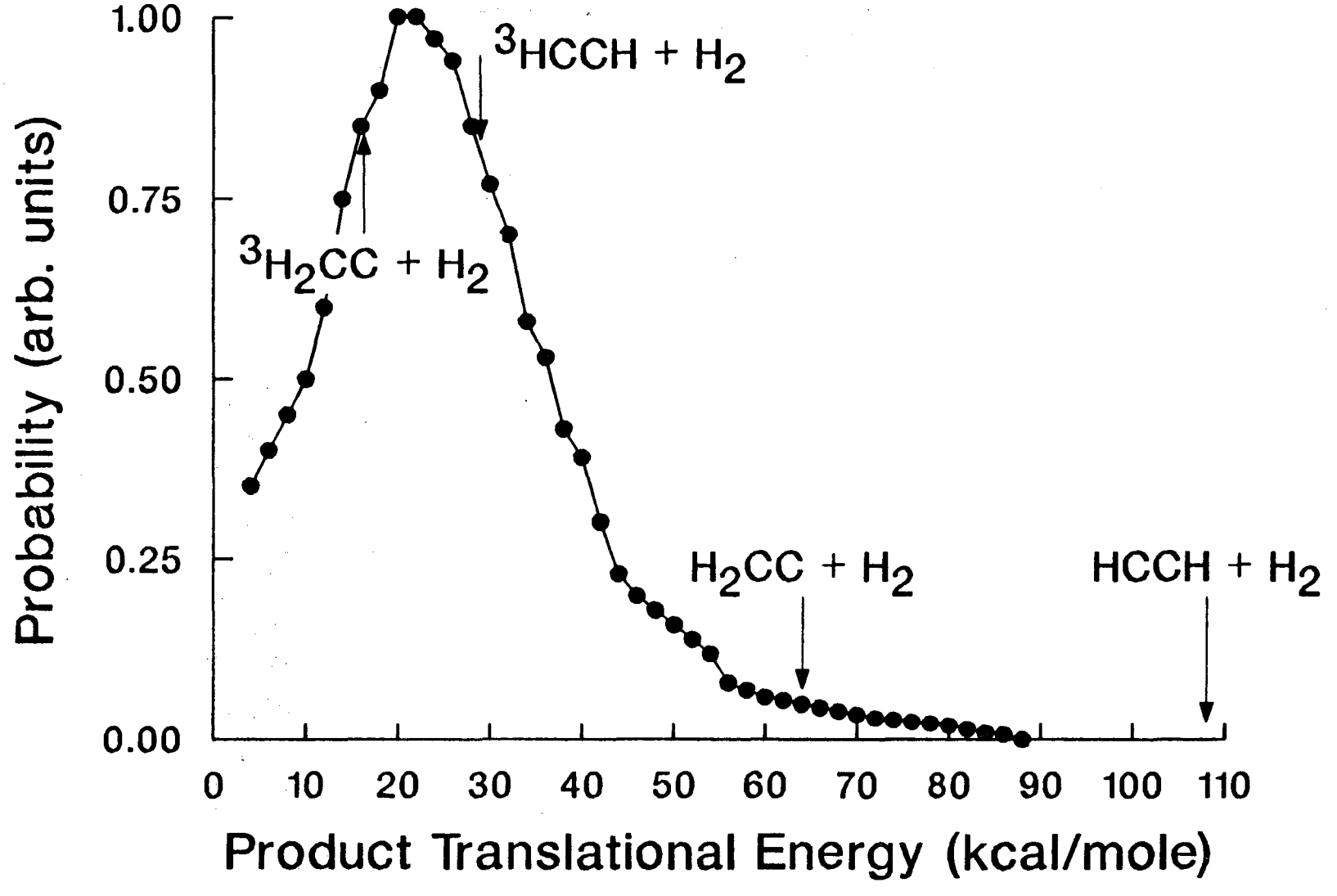
1.00
0.75
0.50
0.25
0.00
Probability (arb. units)
$^3HCCH + H_2$
$^3H_2CC + H_2$
$H_2CC + H_2$
HCCH + H_2
0
10
20
30
40
50
60
70
80
90
100
110
Product Translational Energy (kcal/mole)

Figure 3

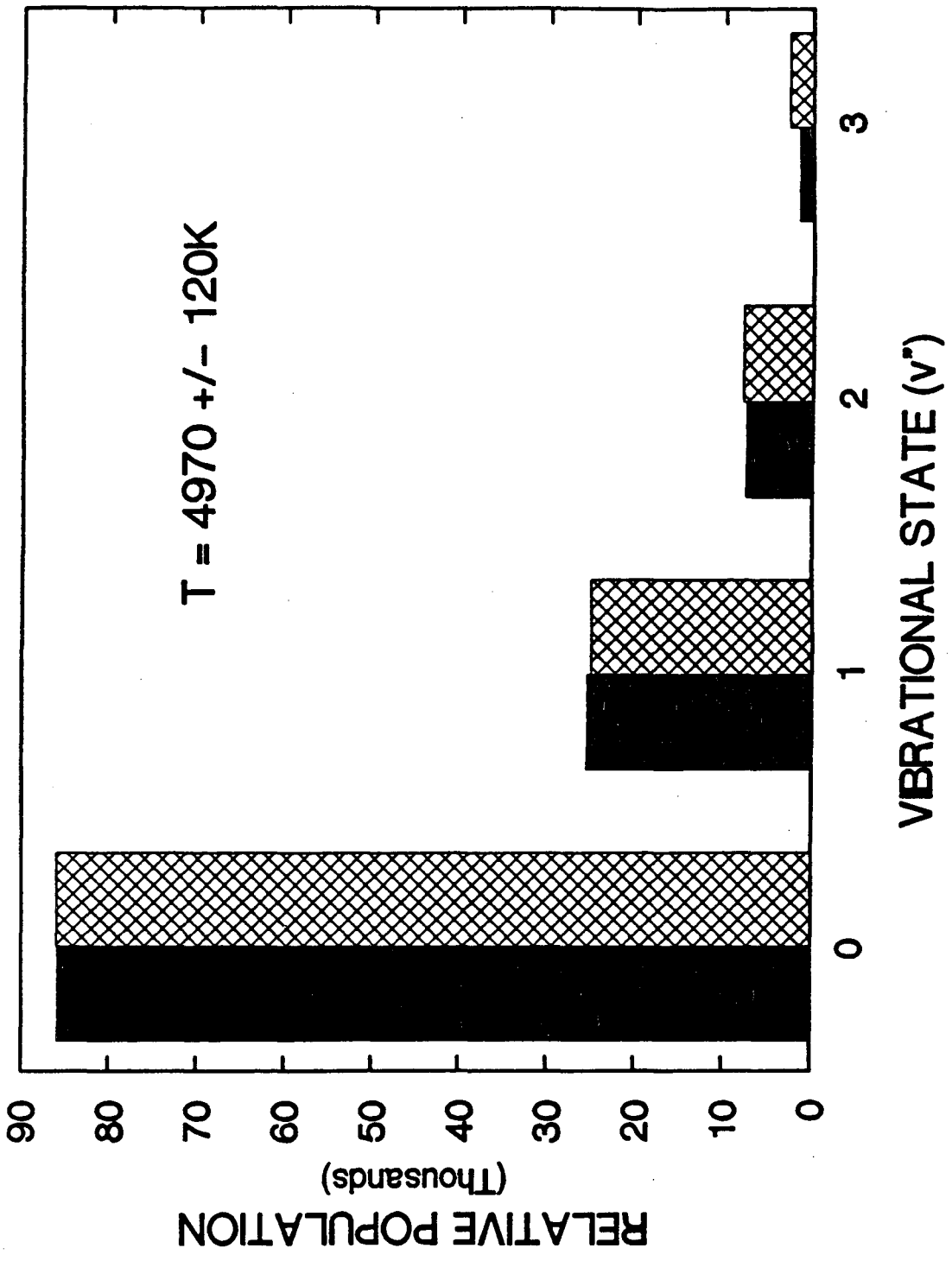
T = 4970 +/- 120K
RELATIVE POPULATION
(Thousands)
0
10
20
30
40
50
60
70
80
90
0
1
2
3
VIBRATIONAL STATE (v")

Figure 4

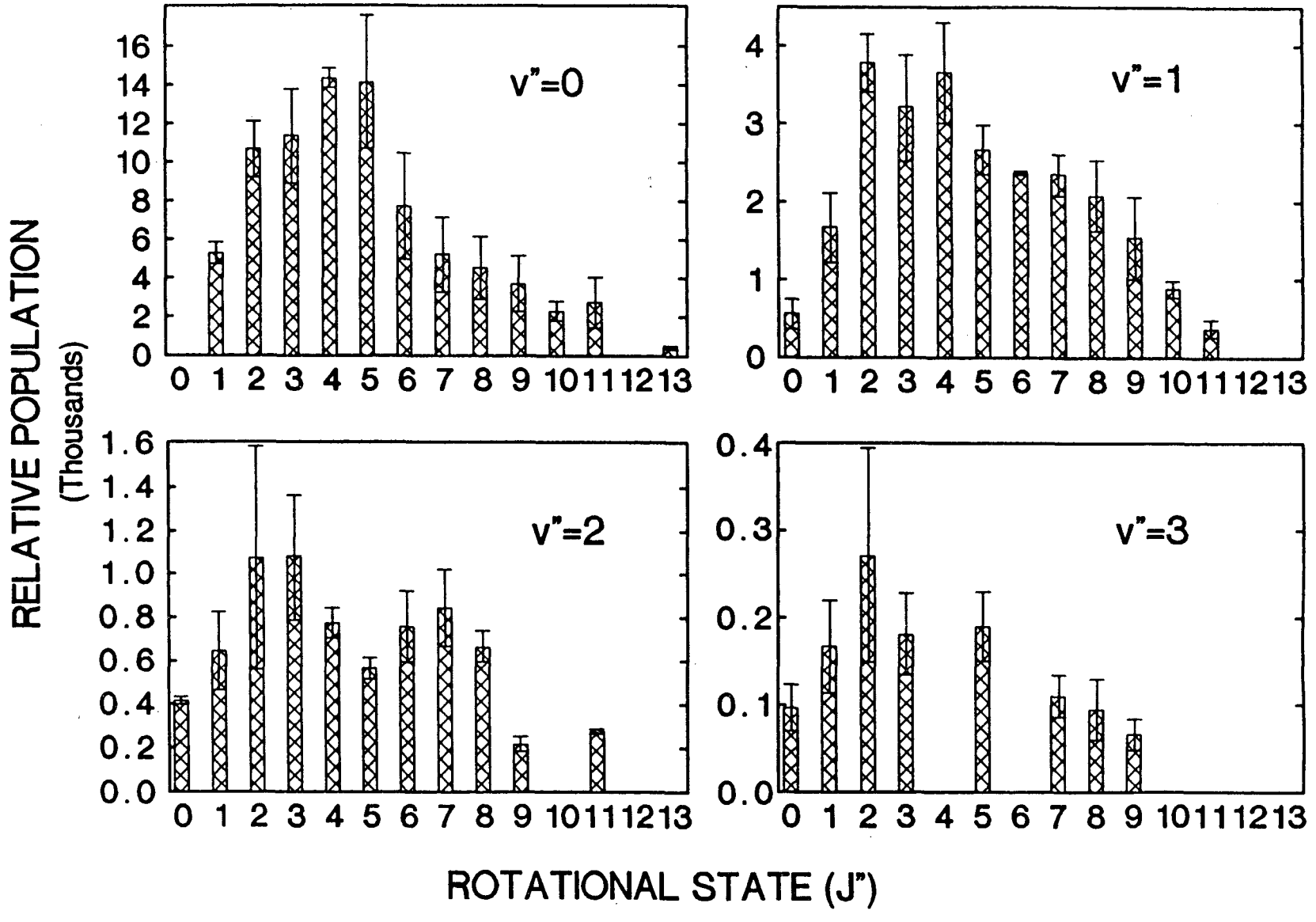
RELATIVE POPULATION
(Thousands)
v"=0
v"=1
v"=2
v"=3
ROTATIONAL STATE (J")

Figure 5

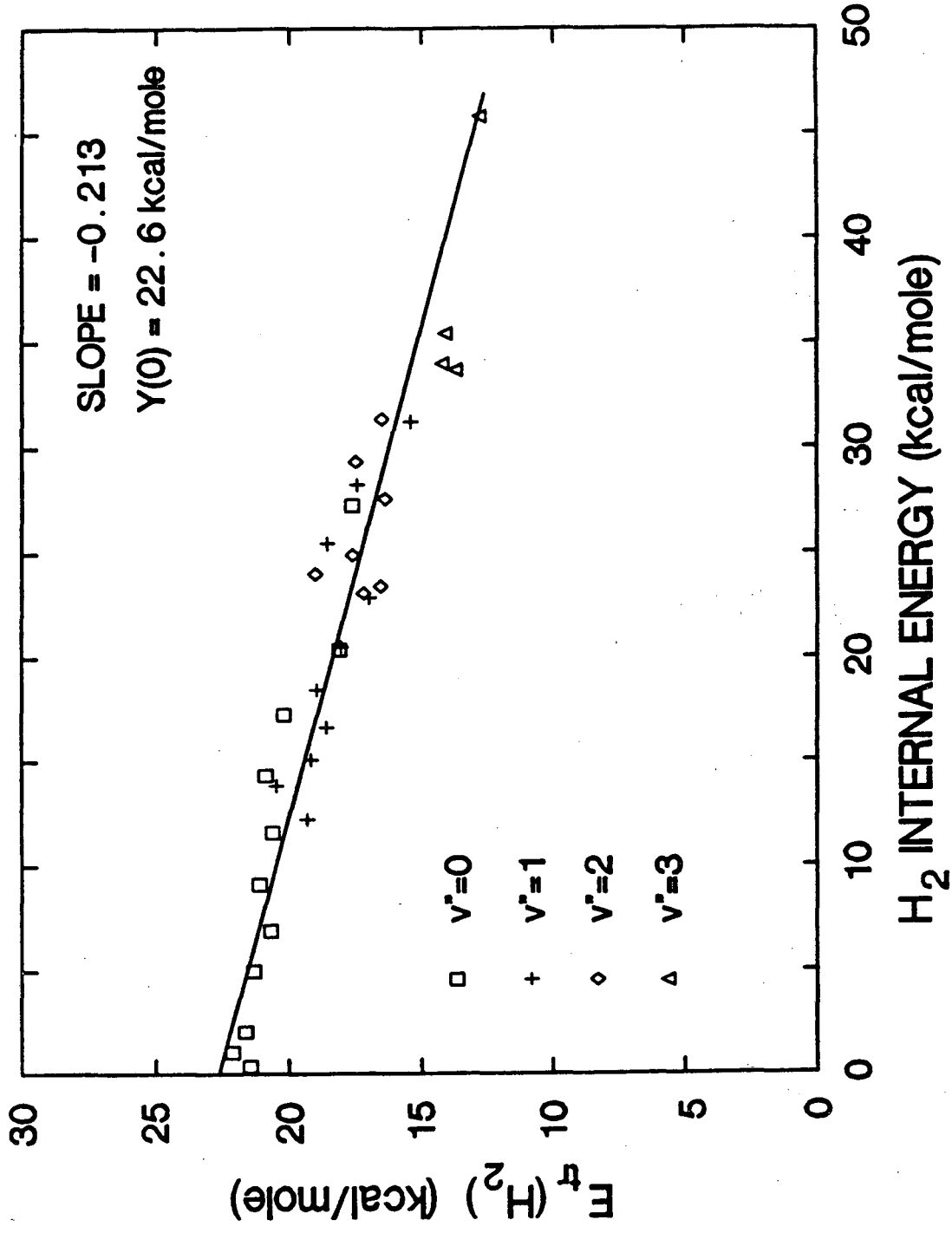
SLOPE = -0.213
Y(0) = 22.6 kcal/mole
v"=0
v"=1
v"=2
v"=3
E_t (H_2) (kcal/mole)
H_2 INTERNAL ENERGY (kcal/mole)
0
5
10
15
20
25
30
0
10
20
30
40
50

Figure 6

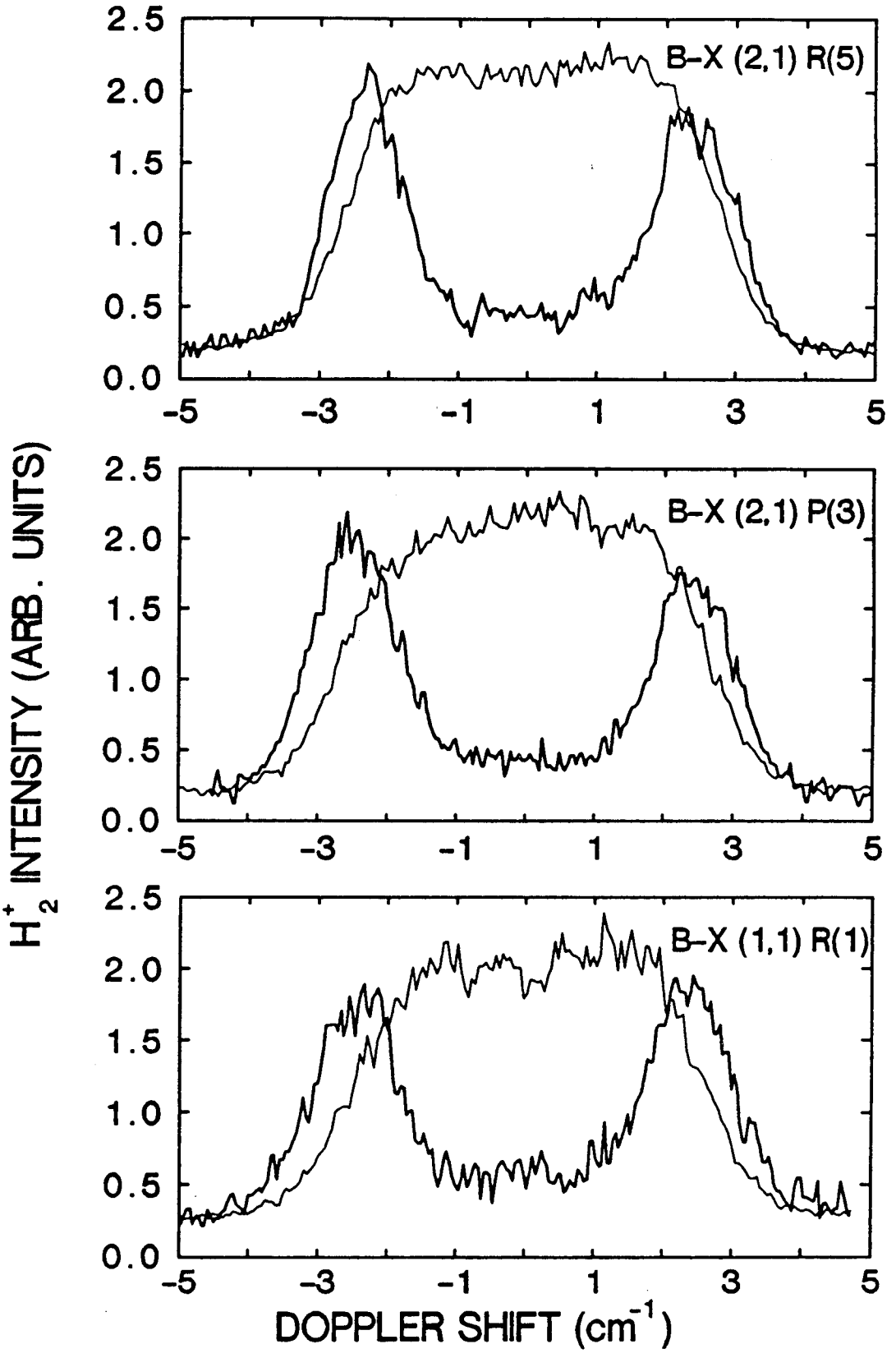
B–X (2,1) R(5)
B–X (2,1) P(3)
B–X (1,1) R(1)
2.5
2.0
1.5
1.0
0.5
0.0
-5
-3
-1
1
3
5
H_2^+ INTENSITY (ARB. UNITS)
DOPPLER SHIFT (cm^{-1})

Figure 7

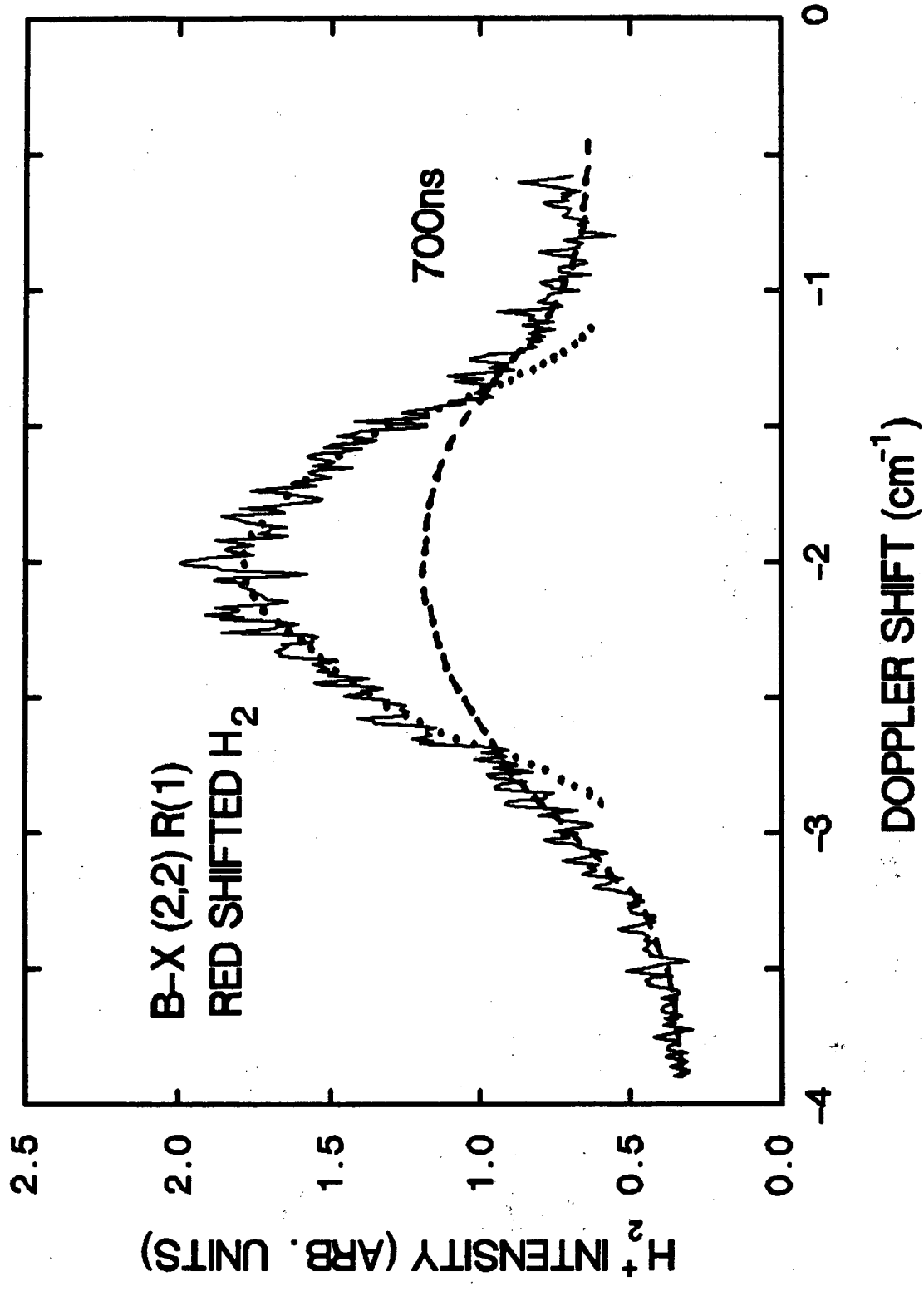
B-X (2,2) R(1)
RED SHIFTED H_2
700ns
H_2^+ INTENSITY (ARB. UNITS)
DOPPLER SHIFT (cm^{-1})
2.5
2.0
1.5
1.0
0.5
0.0
-4
-3
-2
-1
0

Figure 8

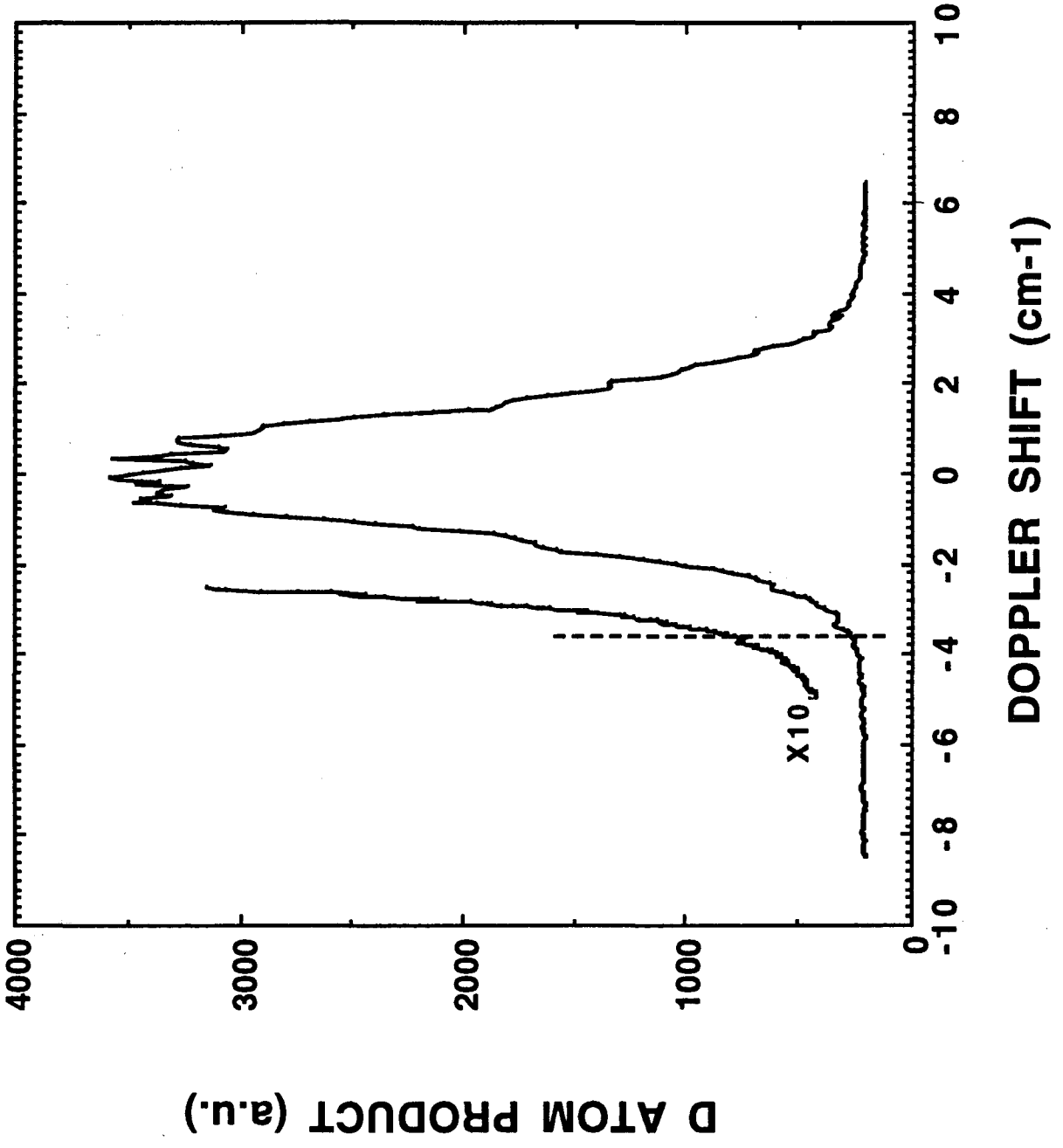
D ATOM PRODUCT (a.u.)
4000
3000
2000
1000
0
-10
-8
-6
-4
-2
0
2
4
6
8
10
DOPPLER SHIFT (cm-1)
X10

Figure 9

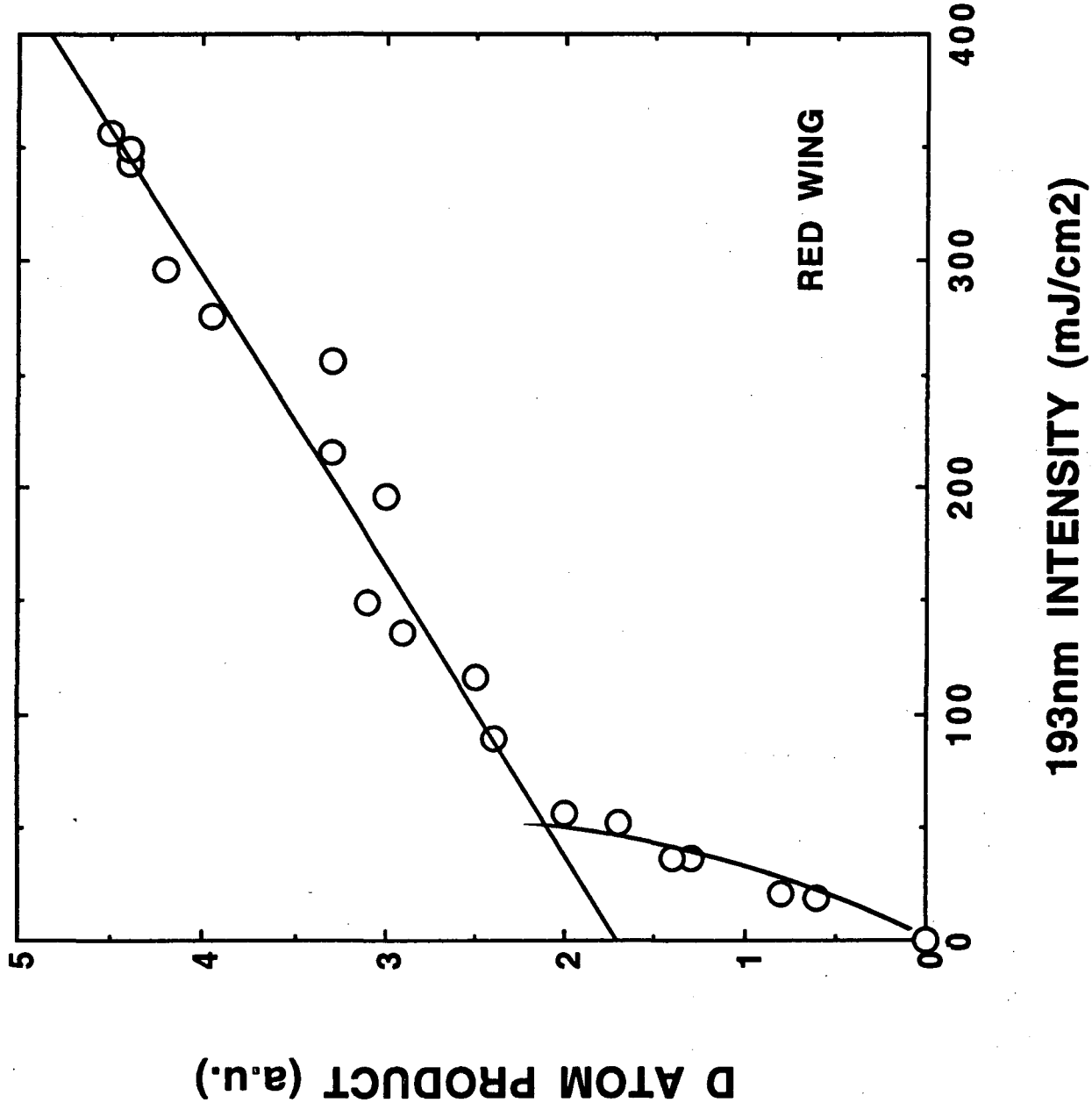
RED WING
D ATOM PRODUCT (a.u.)
193nm INTENSITY (mJ/cm2)
0
1
2
3
4
5
0
100
200
300
400

Figure 10

LAWRENCE BERKELEY LABORATORY
UNIVERSITY OF CALIFORNIA
INFORMATION RESOURCES DEPARTMENT
BERKELEY, CALIFORNIA 94720